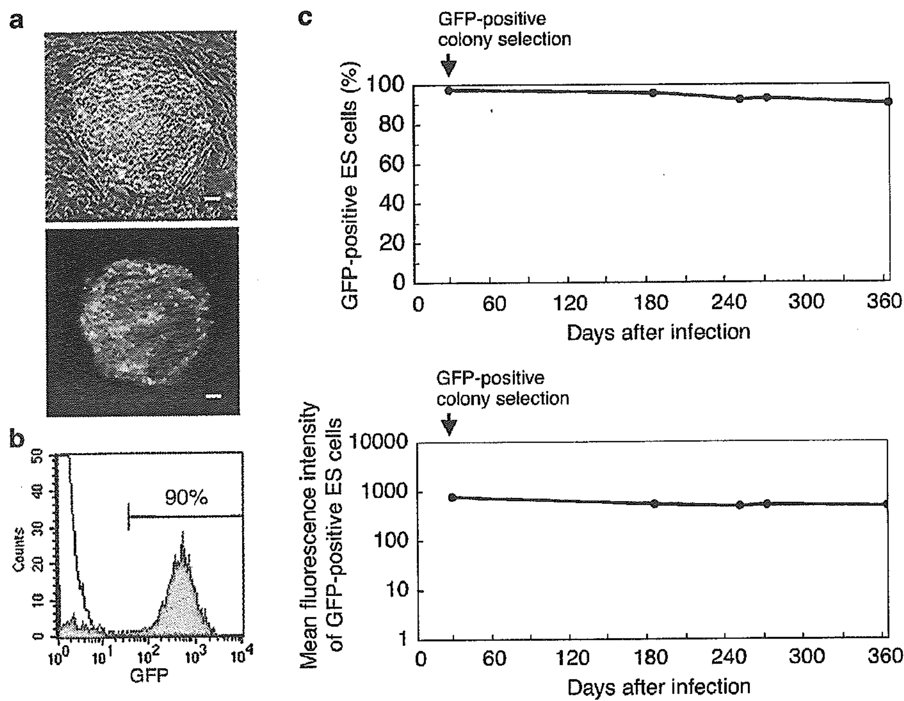

Figure 2 Stable SeV-mediated transgene expression in cynomolgus ES cells. Fluorescent ES cell colonies were plucked under a fluorescent microscope once at 1 month after infection and the cells were further propagated. (a) Phase-contrast (upper) and fluorescence (lower) images of a cynomolgus ES cell colony at day 370 after infection. Bar = 100 μm. (b) Flow cytometric analysis of SeV-infected cynomolgus ES cells at day 370 after infection (shown in green). The percentage of GFP-positive cells is indicated. Uninfected, parental cynomolgus ES cells are indicated by another line (white area). (c) The percentage of GFP-positive cells (upper) and mean fluorescence intensity per GFP-positive cell (lower) after infection with the SeV vector at 10 TU/cell are shown as a function of time (days).

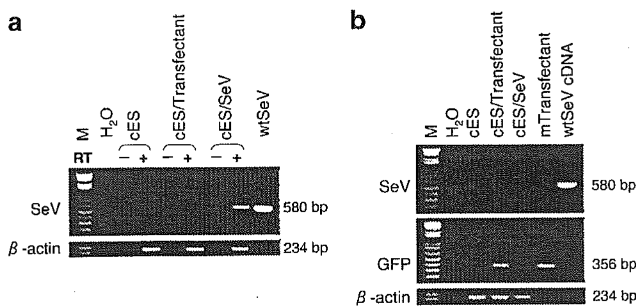

Figure 3 DNA-independent replication and transcription of SeV vector. Total cellular RNA and DNA were extracted from cynomolgus ES cells at day 284 after infection with the SeV vector. RNA-PCR (a) and DNA-PCR (b) for the SeV RNA genome or GFP sequence were conducted. The cynomolgus β-actin sequence was used as an internal control. In the RNA-PCR (a), negative results obtained without reverse transcriptase (designated RT−) confirmed that the amplified products were not derived from cellular DNA. M, 100-kb DNA ladder; cES, naive cynomolgus ES cells; cES/Transfectant, cynomolgus ES cells stably expressing the GFP gene after transfection,[33] cES/SeV, cynomolgus ES cells infected with the SeV vector; wtSeV, wild-type SeV genome; mTransfectant, a GFP-positive mouse cell line after transfection.

diluted out. (iv) The SeV vector is much less unlikely to generate wild-type virus *in vitro* or *in vivo* than oncoretroviral and lentiviral vectors, since homologous recombination between RNA genomes is very rare indeed in negative-strand RNA viruses.[19] (v) The SeV genome is not subject to cellular epigenetic modifications such as methylation, and thus it is unlikely that methylation-based silencing of transgene expression occurs.

No cytotoxic or differentiating effect on ES cells associated with the SeV infection was observed in our study. However, the wild-type SeV contains immunogenic surface proteins, hemagglutinin-neuraminidase (HN) and F proteins, which potentially induce antibody responses.[20,21] For future clinical applications, it would be desired that as many viral genes as possible are deleted from the vector backbone to permit reapplication, improve the safety, and lessen the possible toxicity of SeV vectors. To this end, we have developed a series of attenuated SeV vectors that are F gene-deleted,[6] F gene-deleted with preferable mutations,[22] M gene-deleted,[23] or have deletions of both F and M genes.[24] The modified vectors would be safer for *in vivo* use.

Ribavirin at high concentrations seems toxic to ES cells; presumably, it directly hampers viability and proliferation potential of ES cells. However, we cannot tell whether the observed toxicity is simply due to its toxicity to ES cells, as feeder cells are more highly sensitive to ribavirin than ES cells. In fact, while feeder cells died at 1 mM of ribavirin, cocultured ES cells were alive at this concentration for some time. Cynomolgus ES cells lose pluripotency and proliferation potential without feeder cells. Thus, the observed toxicity to ES cells may also be a secondary event following the injury of feeder cells. Whether the cytotoxicity is primary or secondary, it will be necessary to find modified compounds of less cytotoxicity.

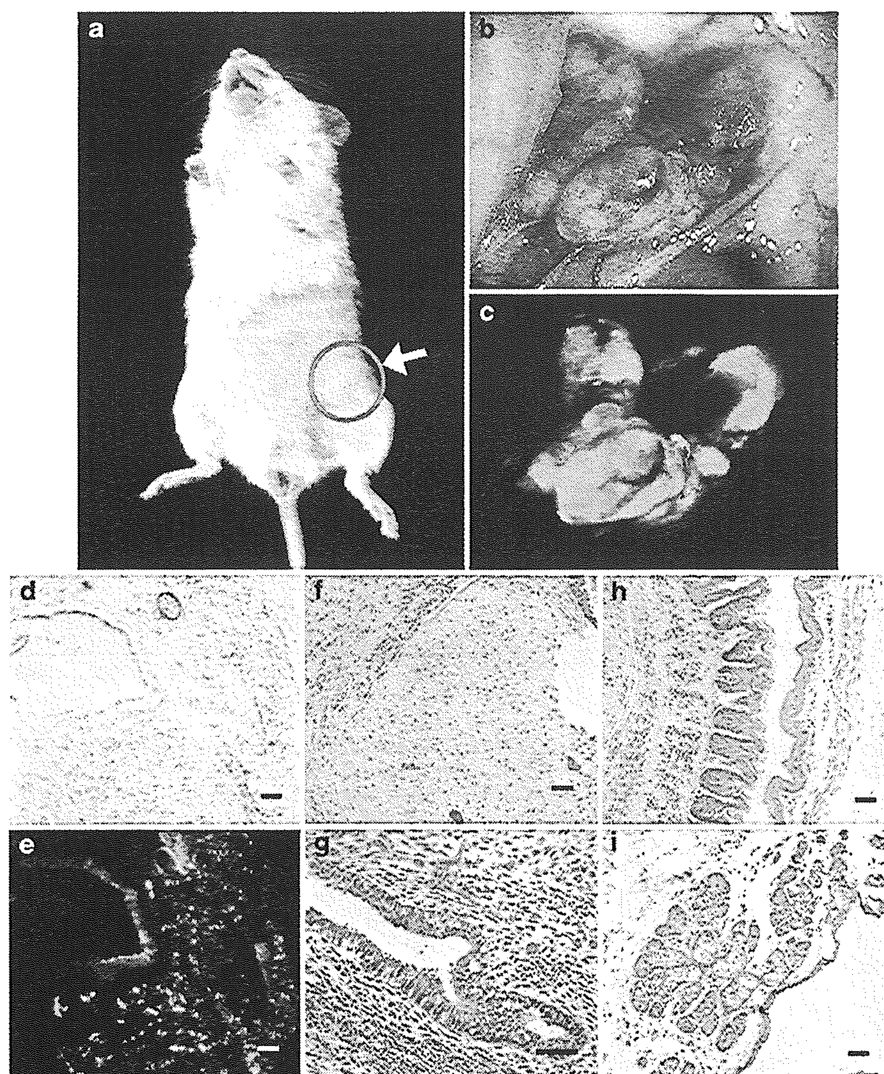

Figure 4 *Pluripotency of SeV-infected cynomlgus ES cells. Tumors formed in NOD-SCID mice after inoculation of the SeV-infected cynomolgus ES cells (a). The tumor was fluorescing ((b), bright field; (c), dark field). Fluorescence was observed uniformly in the tumor under a fluorescent microscope ((d), bright field; (e), dark field). The tumor contained all three embryonic germ layer cells; cartilage (f), ciliated columnar epithelium (g), skin (h), and sebaceous gland (i) (stained with hematoxylin and eosin). Bar = 100 μm.*

Materials and methods

Cell culture

Cynomolgus ES cells (CMK6) were maintained on a feeder layer of mitomycin C (Kyowa, Tokyo, Japan)-treated mouse (BALB/c) embryonic fibroblasts as described previously.[18] The culture medium consisted of Dulbecco's modified Eagle's medium (DMEM)/F12 (Invitrogen, Carlsbad, CA, USA) supplemented with 15% ES cell-qualified fetal calf serum (FCS; Invitrogen), 0.1 mM 2-mercaptoethanol (Sigma, St Louis, MO, USA), 2 mM glutamine (Invitrogen), 0.1 mM nonessential amino acids (Invitrogen), and antibiotics (100 U/ml penicillin and 100 μg/ml streptomycin, Irvine Scientific, Santa Ana, CA, USA). The ES cell colonies were routinely passaged every 3–4 days after dissociation with a combined approach of 0.25% trypsin (Invitrogen) digestion and mechanical cutting. Alkaline phosphatase staining was conducted with an Alkaline Phosphatase Chromogen Kit (Biomeda, Foster City, CA, USA). Embryoid bodies were produced by culturing ES cell aggregates in Petri dishes. LLC-MK2 cells (1×10^6) were grown in six-well plates and cultured in Eagle's minimal essential medium (Invitrogen) supplemented with 10% FCS.

Vectors

The F-defective SeV vector carrying the GFP gene was constructed as previously described.[6] The vector titer was 1.8×10^9 TU/ml determined by counting fluorescent cells after the infection of LLC-MK2 cells. Gene transfer was conducted by adding various concentrations of the SeV vector solution to culture media. After 24 h of incubation, the cells were washed twice with phosphate-buffered saline (PBS) and fresh medium was added. In some experiments, ribavirin (1-β-D-ribofuranosyl-1,2,4-triazole-3-carboxamide; Sigma) was added at various concentrations to the culture media after infection. The

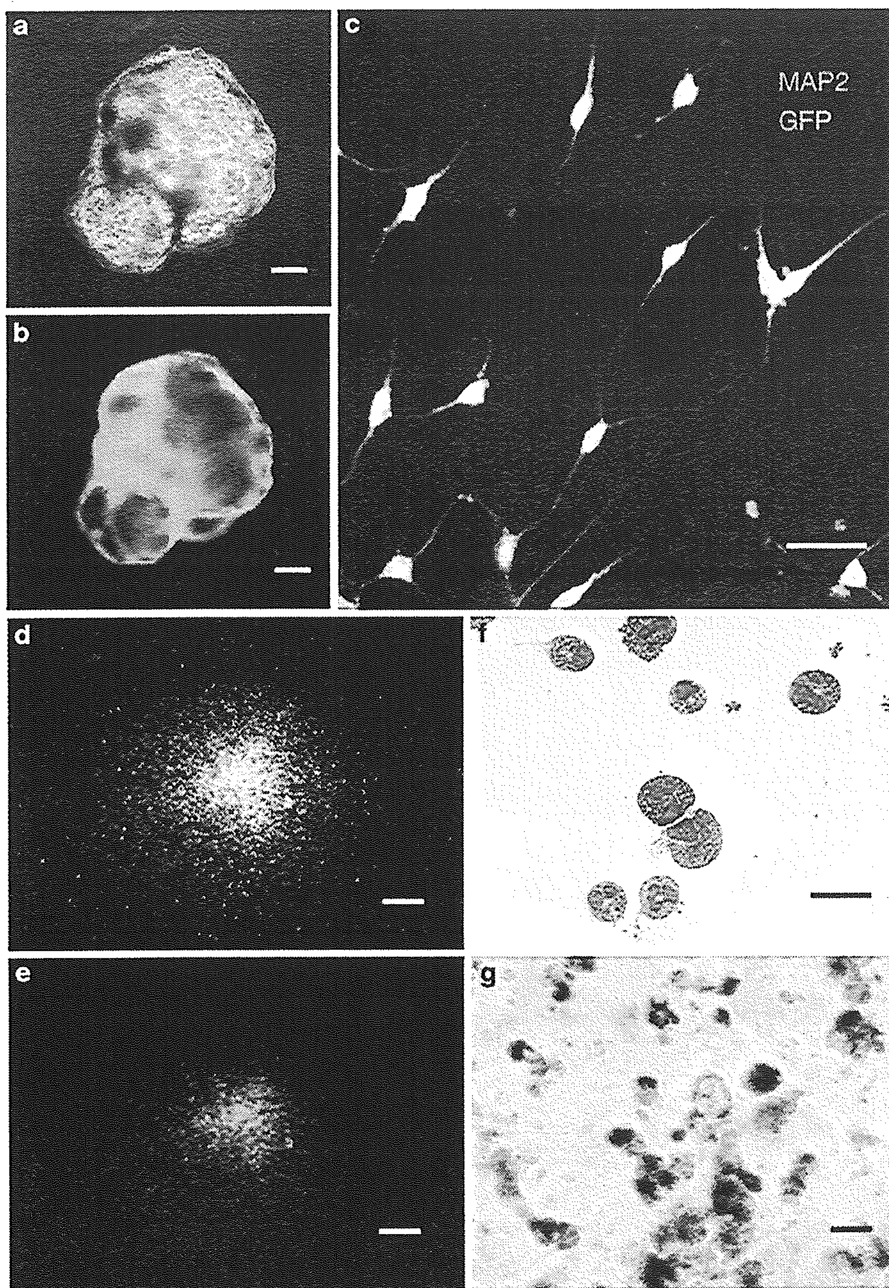

Figure 5 *Stable transgene expression during differentiation. A day-20 cystic embryoid body was observed under a fluorescent phase-contrast microscope, confirming that the embryoid body was fluorescing ((a), bright field; (b), dark field). After infection with the SeV vector, fluorescent cynomolgus ES cells differentiated into neural cells. Double immunostaining with anti-GFP (green) and ant-MAP-2 (red) confirmed that differentiated neural cells expressed GFP (c). Yellow cells indicate GFP-expressing neurons. SeV-infected, fluorescent cynomolgus ES cells also differentiated into fluorescent hematopoietic cells. A clonogenic hematopoietic colony was fluorescing ((d) bright field; (e), dark field). A cytospin specimen of hematopoietic colony cells (Wright–Giemsa staining) showed that the cells were mature granulocytes (f). The infected ES cell-derived, fluorescent neutrophils were positive for NBT (stained in black (g)). Bar = 100 μm (a, b, g); 50 μm (c, f); 500 μm (d, e).*

viral particles in infected cells were quantified by a hemagglutination assay as described previously.[25]

An adenovirus serotype 5-based vector carrying the GFP gene was constructed as reported.[26] It contained the cytomegalovirus (CMV) promoter, simian virus (SV)-40 intron, and SV-40 polyadenylation signal. An AAV serotype 2-based vector expressing the GFP gene under the control of the chicken β-actin promoter with the CMV immediate-early enhancer (a gift from Dr J Miyazaki) was prepared as described previously.[27] Gene transfer experiments were performed using 3.4×10^2 genome copies (g.c.)/cell of the adenoviral vector or 2.4×10^4 g.c./cell of the AAV vector. The period of exposure was 48 h.

Flow cytometry

GFP and SSEA-4 expression was analyzed on a FACScan (Becton Dickinson, Franklin Lakes, NJ, USA) using the

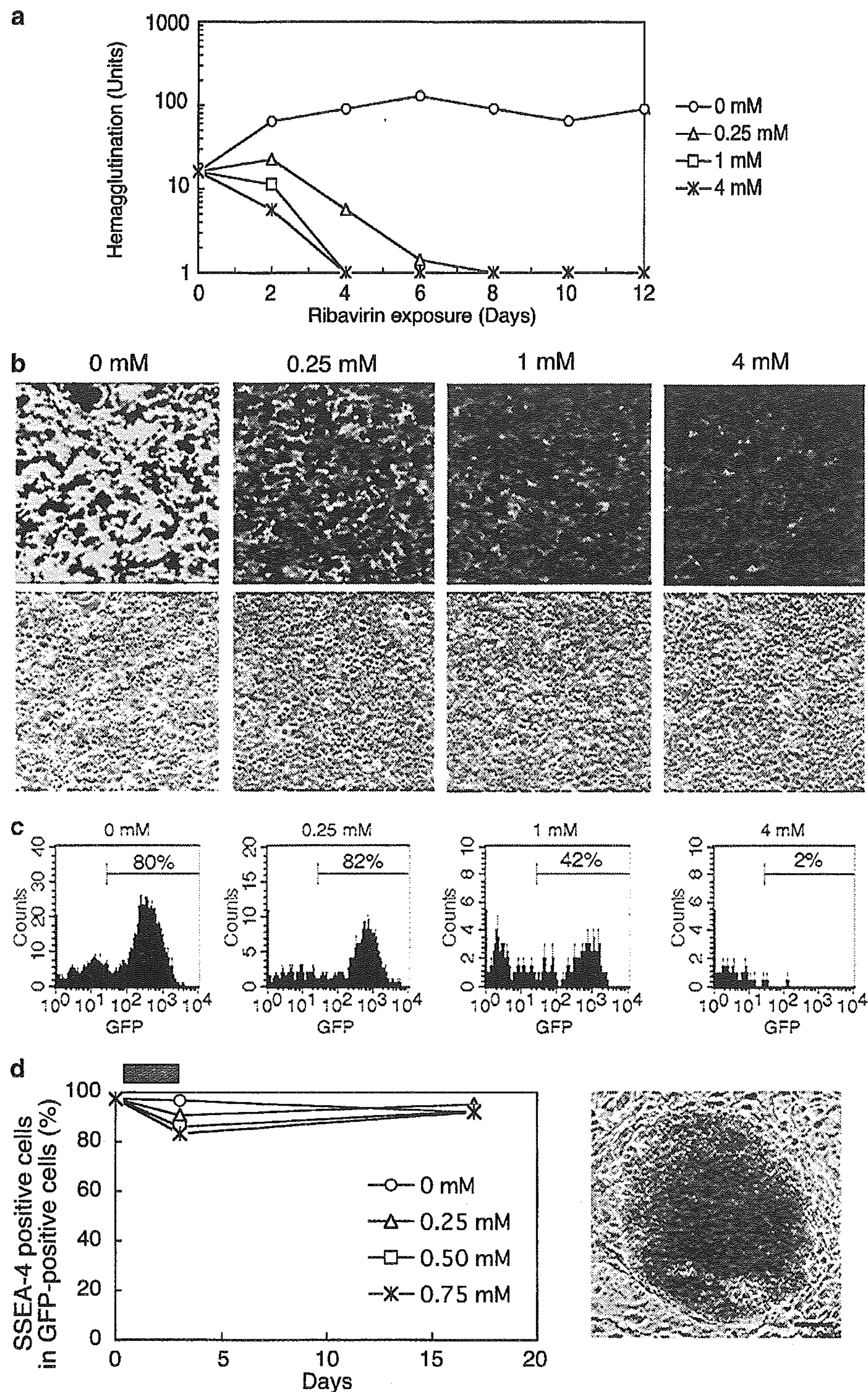

Figure 6 Ribavirin-regulated transgene expression. (a) A rhesus kidney cell line (LLC-MK2) was infected with the SeV vector at 3 TU/cell. Ribavirin was started at various concentrations on day 2 after the infection. The formation of viral particles in the infected LLC-MK2 cells was examined by the hemagglutination assay. (b) The ribavirin-treated LLC-MK2 cells were observed under a fluorescent microscope after an 8-day exposure of ribavirin (upper, dark field; lower, bright field). (c) Ribavirin was added at various concentrations to the SeV-infected, fluorescent cynomolgus ES cells. The GFP expression was assessed by flow cytometry after a 3-day exposure of ribavirin. (d) The fractions of SSEA-4-positive ES cells were assessed by flow cytometry with anti-SSEA-4 before and after a 3-day exposure of ribavirin and are shown as a function of time (days) in the left panel. A gray bar indicates ribavirin treatment. ES cells were stained for alkaline phosphatase (in red) at day 21 after a 3-day exposure of 0.75 mM ribavirin and are shown in the right panel. Bar = 100 μm.

CellQuest software (Becton Dickinson). For SSEA-4 staining, cells were incubated with a primary antibody, anti-SSEA-4 (MC-813-70; Chemicon, Temecula, CA, USA), and then a secondary antibody, PE-conjugated F(ab')2 fragment of rabbit anti-mouse immunoglobulins (DakoCytomation, Glostrup, Denmark). Cocultured BALB/c feeder cells could be distinguished from cynomolgus ES cells by using PE-conjugated anti-mouse

H-2d (SF1-1.1; PharMingen, San Diego, CA, USA), which does not react to cynomolgus cells but does react to BALB/c cells.

Teratoma formation

Cynomolgus ES cells (approximately 10^6 cells per site) were injected subcutaneously into the hind leg of 6- to 8-week-old nonobese diabetic/severe combined immunodeficient mice (Jackson Laboratory, Bar Harbor, ME, USA). The resulting tumors (usually 9–12 weeks after the injection) were dissected and fixed in 4% paraformaldehyde. For histological analysis, samples from the tumors were embedded in paraffin and stained with hematoxylin and eosin. To observe GFP fluorescence, samples were embedded in OTC compound (Sakura, Zoeterwoude, Netherlands), frozen, sectioned, and examined under a fluorescence microscope.

Hematopoietic differentiation

The mouse bone marrow stromal cell line OP9 was maintained in α-modified minimum essential medium (Invitrogen) supplemented with 20% FCS as described previously.[28] For induction of hematopoietic differentiation, ES cells were seeded onto a mitomycin C-treated confluent OP9 cell layer in six-well plates. Medium to support the differentiation was described elsewhere.[29] Cells at day 18 were placed in Methocult GF+ media (StemCell Technologies, Vancouver, Canada) at 1×10^4 and 1×10^5 cells per plate and clonogenic hematopoietic colonies were produced. After 14 days, individual colonies were removed and spun onto glass slides. Cells were stained with the Wright–Giemsa method. The nitro blue tetrazolium (NBT, Sigma) reduction test was performed on the cells as a granulocyte functional assay according to a previously described method.[30]

Neural differentiation

The induction of neural differentiation was carried out as described previously.[31] Day-4 embryoid bodies were plated onto tissue culture dishes and nestin-positive cells were selected in DMEM/F12 medium supplemented with 5 μg/ml of insulin (Sigma), 50 μg/ml of transferrin (Sigma), 30 nM selenium chloride (Sigma), and 5 μg/ml of fibronectin (Sigma) for 5 days. Cells were then trypsinized and plated in polyornithine-coated dishes (15 μg/ml) and expanded in N2 medium[32] supplemented with 1 μg/ml of laminin (Sigma) and 10 μg/ml of basic fibroblast growth factor (bFGF; Roche, Basel, Switzerland) for 6 days. Differentiation was induced by removal of bFGF. To confirm the neural differentiation, cells were stained with anti-human MAP-2. Briefly, cells were fixed in 4% paraformaldehyde in PBS and incubated with anti-human MAP-2 (HM-2; Sigma; diluted 1:4000) and then by Alexa Fluor 594-labeled antibody (diluted 1:500; Molecular Probe, Eugene, OR, USA). The samples were examined under a fluorescence microscope.

DNA-PCR

DNA-PCR for the SeV genome and GFP sequences was carried out as follows. DNA was extracted using the QIAamp DNA mini kits (Qiagen, Hilden, Germany) and 250 ng was used for each PCR with ExTaq (Takara, Shiga, Japan). Amplification conditions were 30 cycles of 94°C for 1 min, a variable annealing temperature (noted below) for 1 min, and 72°C for 1 min. The amplified products were run on 2% agarose gel and visualized by ethidium bromide staining. Primer sequences, annealing temperatures and product sizes were as follows: the SeV vector genome sequence: 5′-AGA GAA CAA GAC TAA GGC TAC C-3′ and 5′-ACC TTG ACA ATC CTG ATG TGG-3′ (55°C, 580 bp); the GFP sequence: 5′-CGT CCA GGA GCG CAC CAT CTT C-3′ and 5′-GGT CTT TGC TCA GGG CGG ACT-3′ (60°C, 356 bp). the cynomolgus β-actin sequence: 5′-CAT TGT CAT GGA CTC TGG CGA CGG-3′ and 5′-CAT CTC CTG CTC GAA GTC TAG GGC-3′ (60°C, 234 bp).

RNA-PCR

RNA-PCR for the SeV RNA genomic sequence was carried out as follows. Total RNA was extracted using RNA STAT-60 (Tel-Test, Friendswood, TX, USA). Reverse transcription was conducted by using Taqman reverse transcription reagents (Applied Biosystems, Foster City, CA, USA). The product (250 ng) after the reverse transcription was used for the subsequent PCR as described above.

Acknowledgements

Cynomolgus ES cells were provided by Norio Nakatsuji (Kyoto University, Kyoto, Japan), Yasushi Kondo (Tanabe Seiyaku Co. Ltd, Osaka, Japan), and Ryuzo Torii (Shiga University of Medical Science, Shiga, Japan). OP9 cells were provided by Toru Nakano (Osaka University, Osaka, Japan). We thank Yujiro Tanaka and Takayuki Asano for cultivating cynomolgus ES cells and Takeshi Hara for conducting NBT tests. We also thank Natsuko Kurosawa for technical assistance.

References

1 Thomson JA *et al.* Embryonic stem cell lines derived from human blastocysts. *Science* 1998; **282**: 1145–1147.

2 Reubinoff BE *et al.* Embryonic stem cell lines from human blastocysts: somatic differentiation *in vitro*. *Nat Biotechnol* 2000; **18**: 399–404.

3 Asano T *et al.* Highly Efficient gene transfer into primate embryonic stem cells with a simian lentivirus vector. *Mol Ther* 2002; **6**: 162–168.

4 Ma Y *et al.* High-level sustained transgene expression in human embryonic stem cells using lentiviral vectors. *Stem Cells* 2003; **21**: 111–117.

5 Gropp M *et al.* Stable genetic modification of human embryonic stem cells by lentiviral vectors. *Mol Ther* 2003; **7**: 281–287.

6 Li HO *et al.* A cytoplasmic RNA vector derived from nontransmissible Sendai virus with efficient gene transfer and expression. *J Virol* 2000; **74**: 6564–6569.

7 Yonemitsu Y *et al.* Efficient gene transfer to airway epithelium using recombinant Sendai virus. *Nat Biotechnol* 2000; **18**: 970–973.

8 Masaki I *et al.* Recombinant Sendai virus-mediated gene transfer to vasculature: a new class of efficient gene transfer vector to the vascular system. *FASEB J* 2001; **15**: 1294–1296.

9 Shiotani A *et al.* Skeletal muscle regeneration after insulin-like growth factor I gene transfer by recombinant Sendai virus vector. *Gene Therapy* 2001; **8**: 1043–1050.

10 Yamashita A *et al.* Fibroblast growth factor-2 determines severity of joint disease in adjuvant-induced arthritis in rats. *J Immunol* 2002; **168**: 450–457.

11 Ikeda Y *et al.* Recombinant Sendai virus-mediated gene transfer into adult rat retinal tissue: efficient gene transfer by brief exposure. *Exp Eye Res* 2002; **75**: 39–48.
12 Jin CH *et al.* Recombinant Sendai virus provides a highly efficient gene transfer into human cord blood-derived hematopoietic stem cells. *Gene Therapy* 2003; **10**: 272–277.
13 Crotty S *et al.* The broad-spectrum antiviral ribonucleoside ribavirin is an RNA virus mutagen. *Nat Med* 2000; **6**: 1375–1379.
14 Vo NV, Young KC, Lai MM. Mutagenic and inhibitory effects of ribavirin on hepatitis C virus RNA polymerase. *Biochemistry* 2003; **42**: 10462–10471.
15 McHutchison JG *et al.* Interferon alfa-2b alone or in combination with ribavirin as initial treatment for chronic hepatitis C. Hepatitis Interventional Therapy Group. *N Engl J Med* 1998; **339**: 1485–1492.
16 Davis GL *et al.* Interferon alfa-2b alone or in combination with ribavirin for the treatment of relapse of chronic hepatitis C. International Hepatitis Interventional Therapy Group. *N Engl J Med* 1998; **339**: 1493–1499.
17 McCormick JB *et al.* Lassa fever. Effective therapy with ribavirin. *N Engl J Med* 1986; **314**: 20–26.
18 Suemori H *et al.* Establishment of embryonic stem cell lines from cynomolgus monkey blastocysts produced by IVF or ICSI. *Dev Dyn* 2001; **222**: 273–279.
19 Spann KM, Collins PL, Teng MN. Genetic recombination during coinfection of two mutants of human respiratory syncytial virus. *J Virol* 2003; **77**: 11201–11211.
20 Tozawa H *et al.* Neutralizing activity of the antibodies against two kinds of envelope glycoproteins of Sendai virus. *Arch Virol* 1986; **91**: 145–161.
21 Tashiro M, Tobita K, Seto JT, Rott R. Comparison of protective effects of serum antibody on respiratory and systemic infection of Sendai virus in mice. *Arch Virol* 1989; **107**: 85–96.
22 Inoue M *et al.* Nontransmissible virus-like particle formation by F-deficient Sendai virus is temperature sensitive and reduced by mutations in M and HN proteins. *J Virol* 2003; **77**: 3238–3246.
23 Inoue M *et al.* A new Sendai virus vector deficient in the matrix gene does not form virus particles and shows extensive cell-to-cell spreading. *J Virol* 2003; **77**: 6419–6429.
24 Inoue M *et al.* Recombinant Sendai virus vectors deleted in both the matrix and the fusion genes: efficient gene transfer with preferable properties. *J Gene Med*, published online 5 May 2004. doi:10.1002/jgm.597.
25 Kato A *et al.* Initiation of Sendai virus multiplication from transfected cDNA or RNA with negative or positive sense. *Genes Cells* 1996; **1**: 569–579.
26 Okada T *et al.* Efficient directional cloning of recombinant adenovirus vectors using DNA–protein complex. *Nucleic Acids Res* 1998; **26**: 1947–1950.
27 Okada T *et al.* Adeno-associated viral vector-mediated gene therapy of ischemia-induced neuronal death. *Methods Enzymol* 2002; **346**: 378–393.
28 Nakano T, Kodama H, Honjo T. Generation of lymphohematopoietic cells from embryonic stem cells in culture. *Science* 1994; **265**: 1098–1101.
29 Li F *et al.* Bone morphogenetic protein 4 induces efficient hematopoietic differentiation of rhesus monkey embryonic stem cells *in vitro*. *Blood* 2001; **98**: 335–342.
30 Sekhsaria S *et al.* Peripheral blood progenitors as a target for genetic correction of $p47^{phox}$-deficient chronic granulomatous disease. *Proc Natl Acad Sci USA* 1993; **90**: 7446–7450.
31 Lee SH *et al.* Efficient generation of midbrain and hindbrain neurons from mouse embryonic stem cells. *Nat Biotechnol* 2000; **18**: 675–679.
32 Johe KK *et al.* Single factors direct the differentiation of stem cells from the fetal and adult central nervous system. *Genes Dev* 1996; **10**: 3129–3140.
33 Takada T *et al.* Monkey embryonic stem cell lines expressing green fluorescent protein. *Cell Transplant* 2002; **11**: 631–635.

Antiviral Chemistry & Chemotherapy 16:363–373

A novel small molecular weight compound with a carbazole structure that demonstrates potent human immunodeficiency virus type-1 integrase inhibitory activity

Hua Yan[1], Tomoko Chiba Mizutani[1], Nobuhiko Nomura[2], Tadakazu Takakura[2], Yoshihiro Kitamura[3], Hideka Miura[1], Masako Nishizawa[1], Masashi Tatsumi[1], Naoki Yamamoto[1] and Wataru Sugiura[1*]

[1]AIDS Research Center, National Institute of Infectious Diseases, Tokyo, Japan
[2]Research and Discovery Laboratories, Toyama Chemical Co. Ltd., Toyama, Japan
[3]Division of Infectious Diseases, Advanced Clinical Research Center, Institute of Medical Science, University of Tokyo, Japan.

*Corresponding author: Tel: +81 42 561 0771; Fax: +81 42 561 7746; E-mail: wsugiura@nih.go.jp

The integration of reverse transcribed proviral DNA into a host genome is an essential event in the human immunodeficiency virus type 1 (HIV-1) replication life cycle. Therefore, the viral enzyme integrase (IN), which plays a crucial role in the integration event, has been an attractive target of anti-retroviral drugs. Several IN inhibitory compounds have been reported previously, yet none has been successful in clinical use. To find a new, more successful IN inhibitor, we screened a diverse library of 12 000 small molecular weight compounds randomly by *in vitro* strand-transfer assay. We identified a series of substituted carbazoles that exhibit strand-transfer inhibitory activity at low micromolar concentrations. Of these, the most potent compound exhibited an IC_{50} of 5.00 ±3.31 µM (CA-0). To analyse the structural determinants of strand-transfer inhibitory activity of the carbazole derivatives, we selected 23 such derivatives from our compound library and performed further analyses. Of these 23 compounds, six showed strong strand-transfer inhibition. The inhibition kinetics analyses and ethidium bromide displacement assays indicated that the carbazole derivatives are competitive inhibitors and not intercalators. An HeLa4.5/LTR-nEGFP cell line was employed to evaluate *in vitro* virus replication inhibition of the carbazole derivatives, and IC_{50} levels ranged from 0.48–1.52 µM. Thus, it is possible that carbazole derivatives, which possess structures different from previously-reported IN inhibitors, may become novel lead compounds in the development of IN inhibitors.

Keywords: integrase inhibitor, carbazole, HIV-1, antiretroviral drug

Introduction

Human immunodeficiency virus type 1 (HIV-1), causative agent of acquired immunodeficiency syndrome (AIDS), possesses three critical enzymes for replication. These are protease (PR), reverse transcriptase (RT), and integrase (IN) (Ruscetti, 1985; Kohl *et al.*, 1988; LaFemina *et al.*, 1992). As inactivating any of these enzymes may negate the infectivity of HIV-1, the enzymes have been targets of anti-retroviral drug development. Indeed, great progress in anti-retroviral drug discovery has been achieved in recent decades, and today 10 RT inhibitors and eight PR inhibitors (De Clercq, 1992; Troncher & Seman, 2003; Balzarini, 2004; Imamichi, 2004) are available for anti-retroviral treatments. The third enzyme, IN, has also been a major target of inhibitor development. L-708,906 and L-731,988, which possess diketo acid moieties within their structures, were the first IN-specific inhibitors discovered (Pommier *et al.*, 2000; Dayam & Neamati, 2003; Pluymers *et al.*, 2002; Hazuda *et al.*, 2000). S-1360 and L-870,810, which also have diketo acid moieties, are IN inhibitors that have reached clinical Phase I/II trials for the first time (Johnson *et al.*, 2004; Hazuda *et al.*, 2004). However, although there have been large advances in the development of IN inhibitors, further research and analysis is required to develop clinically usable compounds.

Integrase (IN), the leading target of novel anti-retroviral inhibitor development, is the enzyme responsible for integration, wherein reverse transcribed HIV-DNA is inserted into a host genome, and is critical for viral replication, which in turn establishes latency and chronic infection (Chun *et al.*, 1995). IN is composed of three distinct

©2005 International Medical Press

domains – the N-terminal domain (amino acids 1–50) with a zinc-binding motif (Schauer & Billich, 1992; Burke *et al.*, 1992), the catalytic core domain (amino acids 50–212) with polynucleotidyl transfer activity and sequence-specific endonuclease activity (Engelman & Craigie, 1992; Engelman *et al.*, 1994) and the C-terminal domain (amino acids 212–288), which has been thought to relate to nonspecific DNA binding (Khan *et al.*, 1991; Woerner & Marcus-Sekura, 1993).

At present, the function and structure of each domain has not been fully understood. The most well-analysed domain is the catalytic core domain, and its active site has highly conserved amino acidic residues Asp64, Asp116 and Glu152, which are critical for polynucleotidyl transfer activity (LaFemina *et al.*, 1992; Engelman *et al.*, 1995). Previously reported potent IN inhibitors L-708,906, L-731,988, L-801,810, S-1360 and 5-CITEP are all targeted to this domain. These inhibitors bind to the active site, displace divalent metal ion Mg^{2+} from the active site and inactivate the catalytic activity of IN (Grobler *et al.*, 2002; Dayam & Neamati, 2003; Goldgur *et al.*, 1999; Johnson *et al.*, 2004). No specific inhibitors have been reported for the N-terminal and C-terminal domains.

In the present study we attempted to identify novel IN inhibitory compounds, and therefore we conducted a random screening of a library of small molecular weight compounds. As a result, we discovered a series of novel IN inhibitory compounds with carbazole structures, that are quite different from previously reported inhibitory compounds.

Materials and methods

Preparation of integrase

The sequence coding the NL4-3 integrase (IN) was cloned into pET28b(+) (Novagen, Madison, WI, USA), generating pET-IN that codes NL4-3 IN with a hexa-histidine tag at the N-terminus. *Escherichia coli* strain Rosetta (DE3) (Novagen) transformed with pET-IN was grown in 1 l of Super Broth (Biofluids, Camarillo, CA, USA) containing 100 μg/ml kanamycin at 30°C until the optical density of the culture had reached between 0.5 and 0.7 at 600 nm. The recombinant protein expression was induced by isopropyl-1-thio-D-galactopyranoside. After incubation for 3 h, the cells were harvested and resuspended in 100 ml of preparation buffer (20 mM Tris-HCl, pH 8.0, 0.5 M NaCl) and disrupted by sonication. Following high-speed centrifugation at 40 000×g for 45 min at 4°C, the pellet was homogenized in GBB buffer (50 mM Tris-HCl, pH 8.0, 6 M Guanidine HCl and 2 mM 2-ME). The residual pellet was again sonicated and centrifuged at 40 000×g for 30 min at 4°C.

The supernatant was filtered through a 0.22 μm filter and mixed with 1 ml of nickel-affinity resin (Sigma, St. Louis, MO, USA), and incubated overnight at 4°C. The resin was washed twice by mixing with 20 ml of GBB containing 5 mM imidazole (Sigma). The protein was eluted with GBB containing 1 M imidazole. The fractions containing integrase were pooled and 0.5 M EDTA was added to a final concentration of 5 mM. This eluted protein was then sequentially dialysed against (i) 6 M guanidine HCl, 50 mM Tris-HCl (pH 8.0), 2 mM 2-ME, 1 mM EDTA for 2 h at room temperature, (ii) 6 M guanidine HCl, 50 mM Tris-HCl (pH 8.0), 10 mM DTT, 1 mM EDTA for 16 h at room temperature, (iii) 4 M urea, 50 mM Tris-HCl (pH 8.0), 0.5 M NaCl, 1 mM DTT, 0.1 mM EDTA for 16 h at 4°C, (iv) 2 M urea, 50 mM Tris-HCl (pH 8.0), 0.5 M NaCl, 1 mM DTT, 0.1 mM EDTA, 20% (w/v) glycerol for 16 h at 4°C, (v) 1 M urea, 50 mM Tris-HCl (pH 8.0), 1 M NaCl, 1 mM DTT, 0.1 mM EDTA, 15 mM 3-[(3-cholamidopropyl) dimethylammonio]-1-propanesulfonate (CHAPS), 20% (w/v) glycerol for 16 h at 4°C, and (vi) 50 mM Tris-HCl (pH 8.0), 1 M NaCl, 1 mM DTT, 0.1 mM EDTA, 15 mM CHAPS, 20% (w/v) glycerol for 16 h at 4°C. The final preparation was stored at −80°C.

The purified enzyme activity was confirmed and evaluated by strand-transfer assay using M8 apparatus (IGEN, Gaithersburg, MD, USA).

Preparation of test compounds

A diverse library of 12 000 small-molecule compounds was supplied by Toyama Chemicals Co. Ltd. (Toyama, Japan). All test compounds were dissolved in DMSO and adjusted to 2 mM concentration. S-1360 was synthesized as positive control for strand transfer assay.

Construction of strand-transfer assay

Two different strand-transfer assay systems were employed in the IN inhibitor screening trial. For the first screening step, an M8 apparatus and strand-transfer assay kit, ORIGEN HIV integrase assay (IGEN), was used. In brief, magnetic beads coated with 29 mer donor double-stranded DNA (dsDNA) were mixed with purified IN (15 pmol), followed by adding the test compound and 20 mer target dsDNA tagged with ruthenium, conducting electronically inducible fluorescence chemistry, and incubating for 1 h at 37°C. Subsequently, the entire reaction solution was applied to the M8 apparatus, and then strand-transfer products were captured by a magnet in the flow-circuit of the equipment. The amount of the strand-transfer product was measured by ruthenium fluorescence activity. For the second and later screening steps, in-house strand-transfer assay was employed. The in-house assay was designed in 96-well plate format to achieve high-throughput screening.

©2005 International Medical Press

The following donor and target DNA oligonucleotides were designed and used:
Donor-1 (D1): 5′-ACTGCTAGAGATTTTCCACACTGACTAAAAG-3′
Donor-2 (D2): Biotin-5′-CTTTTAGTCAGTGTGGAAAATCTCTAGCA-3′
Target-1 (T1): 5′-CTAGAGATTTTCCACACTGACTAAAAG-3′-Digoxigenin (DIG),
Target-2 (T2): 5′-CTTTTAGTCAGTGTGGAAAATCTCTAG-3′-DIG

To form dsDNA, the D1–D2 pair and the T1–T2 pair were mixed in the presence of 0.1 M NaCl and denatured for 10 min at 95°C, followed by an annealing process, gradual cooling down to room temperature. One pmol biotinulated donor dsDNA (D1–D2), 15 pmol IN protein and 5 µl test compounds (100 µM in DMSO) were mixed together in assay buffer (25 mM 3-(N-morpholino)-propanesulfonic acid, pH 7.2, 25 mM NaCl, 10 mM $MgCl_2$, 10 mM DTT, 5% PEG, 10% DMSO), followed by the addition of 0.75 pmol target dsDNA (T1–T2), and adjusted to a final volume of 100 µl and incubated for 1 h at 37°C. After the incubation, the mixture was adjusted to a final volume of 200 µl with ELISA buffer (20 mM Tris [pH 8.0], 0.4 M NaCl, 10 mM EDTA, 0.1 mg/ml sonicated DNA). To harvest the strand-transfer product, the mixture was transferred into a 96-well micro titre plate coated with streptavidin (PIERCE, Rockford, IL, USA), followed by adding an alkaline phosphatase conjugated anti-DIG antibody (Roche Diagnostics, Mannheim, Germany) and a disodium 3-(4-methoxyspiro[1,2-dioxetane-3,2′-(5′-chloro)tricyclo[3.3.1.1^{3,7}]decan]-4-yl) phenyl phosphate (CSPD) substrate (Roche). The lumino-intensity was quantified with a Luminous CT-9000D luminometer (DIA-IATRON, Tokyo, Japan).

In addition to the above two different strand-transfer assays, a strand-transfer assay with radioisotope labelled target DNA and SDS-PAGE was employed in order to visually confirm the strand-transfer inhibition (Craigie *et al.*, 1995). By use of T4 polynucleotide kinase (TAKARA BIO, Osaka, Japan), the 5′ end of 20 mer target oligonucleotide-A (5′-TGTGGAAAATCTCTAGCAGT-3′) was labelled with [γ-^{32}P] ATP (370 MBq/µl, Amersham Bioscience, Tokyo, Japan). After the labelling reaction was terminated by adding EDTA, complementary oligonucleotide-B (5′-ACTGCTAGAGATTTTCCACA-3′) was added, and dsDNA was formed by heat denaturation and gradual cooling to room temperature. Unincorporated [γ-^{32}P]ATP was removed by G-25 Column (Amersham Bioscience, Piscataway, NJ). The reaction products were applied to 20% denatured polyacrylamide gel electrophoresis (300V/25A). The result of the electrophoresis was analysed by BAS-2500 (Fuji film, Tokyo, Japan).

Inhibition kinetics of IN

To analyse the strand-transfer inhibition mechanism of the test compounds, whether the action is competitive inhibition or non-competitive inhibition, Michaelis-Menten constant (K_m) and maximum velocity (V_{max}) were evaluated. Strand-transfer inhibition was evaluated on eight different time points (0, 1, 3, 5, 7.5, 10, 15, and 20 min) with four different compound concentrations (0, 1, 5, 10 µM) and target DNA concentrations (0.167, 0.25, 0.5, and 1 pmol). The initial reaction rate constants of IN were determined by linear regression using linear data points of product concentration–time plots. K_m and V_{max} were calculated from the Y-axis intercept in a plot of the slopes of Lineweaver-Burk analysis.

Intercalative activity evaluation

To clarify the possibility of intercalative activity of test compounds, ethidium bromide (EtBr) displacement assay was carried out following the protocol reported previously (Cain *et al.*, 1978). In brief, 1 µM calf thymus DNA (Invitrogen, Carlsbad, CA, USA) was mixed with EtBr (final concentration at 1.26 µM) and reaction buffer (2 mM HEPES, 10 µM EDTA, 9.4 mM NaCl, pH 7.0), and incubated for 10 min at room temperature. After the incubation, test compounds were added into the calf thymus DNA–EtBr mixture at different concentrations (final concentrations of 0.01–1000 µM). Fluorescence intensity of each mixture was determined by Fluoroskan Ascent FL (Helsinki, Finland. Excited at 544 nm, emitted at 590 nm). Actinomycin D (ICN Biomedical, Aurora, OH, USA), which is known as an intercalator, was employed as the positive control of the assay.

Molecular modelling studies

Molecular modelling studies were carried out using SYBYL software Version 6.9.1 (Tripos, St. Louis, MO, USA) running on an SGI Fuel workstation equipped with 600-MHz R14000 processor (SGI, Mountain View, CA, USA).

Evaluation of *in vitro* antiviral activity

To evaluate HIV-1 replication inhibition by selected test compounds, *in vitro* antiviral assays were performed using a HeLa4.5/nEGFP reporter cell line. The HeLa4.5/nEGFP reporter cell line was established by transfection of CD4 and LTR driven EGFP reporter protein into the HeLa cell line. HeLa4.5/nEGFP reporter cells were maintained with D-MEM (Sigma) containing 5% FCS (Hyclone, Logan, UT, USA), 500 µg/ml G418, 1 µg/ml blasticidin and 2 µg/ml puromycin.

One day before conducting the assay, 1x10^4 HeLa4.5/nEGFP cells were seeded into clear bottom black 96-well plates (NUNC, Rochester, NY, USA) with

200 μl/well medium and incubated at 37°C, 5% CO_2. The next day, 1250 $TCID_{50}$ HXB2 were added in each well, followed by addition of the test compounds in final concentrations of 5, 1, 0.2, 0.04, 0.008, 0.0016, 0.00032, and 0.000064 μM. Forty-eight hours after infection, the cells were fixed by 3.2% formaldehyde and the nuclei of cells were stained by 10 μg/ml Hoechst33342 (Molecular Probes, Engene, OR, USA). EGFP positive cell number ($EGFP^+$) and Hoechst33342 positive cell number ($hoechst33342^+$) were determined by Cellomics Array Scan, HSC Systems (Beckman Coulter, Tokyo, Japan).

Inhibitory activity of each compound was determined by the following formula:

% inhibition = 1 − {($EGFP^+$ cell number with drug/$hoechst33342^+$ cell number with drug) − ($EGFP^+$ cell number without infection/$hoechst33342^+$ cell number without infection)}/{($EGFP^+$ cell number without drug/$hoechst33342^+$ cell number without drug) − ($EGFP^+$ cell number without infection/$hoechst33342^+$ cell number without infection)}.

Results

A small molecule bearing a carbazole moiety demonstrated strand-transfer inhibitory activity

A diverse library of 12 000 small-molecule compounds was screened for strand-transfer inhibitory activity at 100 μM concentration by M8 apparatus. Seventy-two compounds that demonstrated more than 80% strand-transfer-inhibition were selected and applied to the second screening using in-house strand-transfer assay. In the second screening, to confirm dose-dependent inhibition of the test compounds, each compound was tested at four different concentrations. Of the 72 compounds, a compound bearing a carbazole moiety, 8-chloro-2-[2-(dimethylamino)ethyl]-9-hydroxy-5-methylpyrrolo[3,4-c]carbazole-1,3(2H,6H)-dione (coded as CA-0), was found to demonstrate potent strand-transfer inhibitory activity (Figure 1A). As shown in Figure 1B, CA-0 demonstrated clear dose-dependent inhibition of the strand-transfer reaction with an IC_{50} of 5.00 ±3.31 μM. The dose-dependent inhibition was also confirmed by SDS-PAGE with [γ-^{32}P] labelled target DNA. As demonstrated in Figure 1C, strand-transferred product bands diminished along with increased concentration of the inhibitor. IC_{50} value determined from intensities of the bands was 1.24 ±0.09 μM, which was consistent with that evaluated via the plate assay.

Strand-transfer inhibition of 23 carbazole derivatives, and the relationship between their structures and inhibitory activity

To understand the relationship between structure and strand-transfer inhibition activity, we selected 23 carbazole

Figure 1. Structure and strand transfer inhibitory activity of 8-chloro-2-[2-(dimethylamino) ethyl]-9-hydroxy-5-methylpyrrolo[3,4-c]carbazole-1,3(2H,6H)-dione (CA-0)

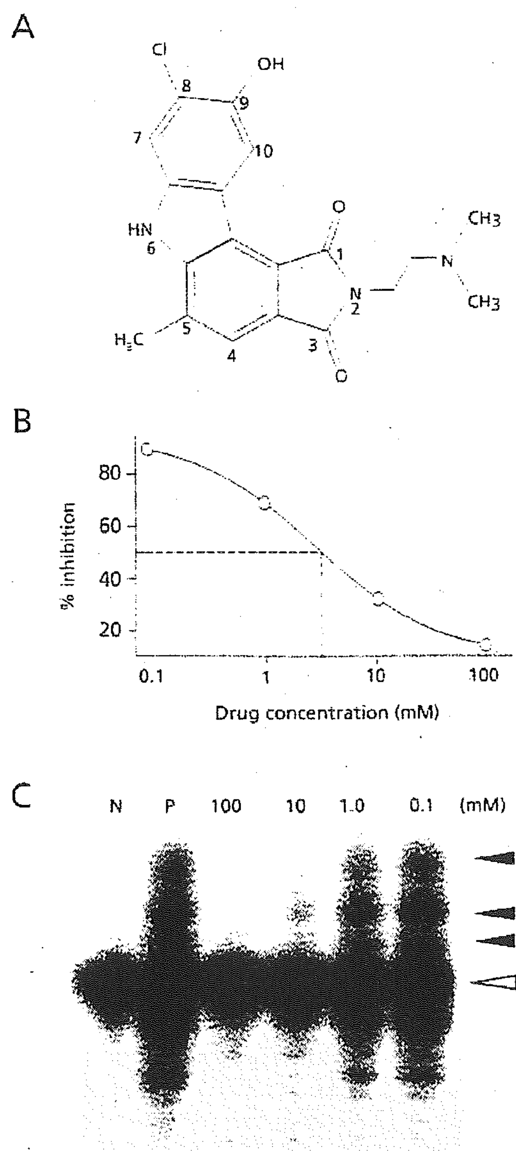

(A) The structure of CA-0, a strand transfer inhibitory compound identified from among a library of 12 000 small molecular weight compounds. It has a carbazole structure as a scaffold. The small numbers written beside the structure indicate the residue number of the compound. (B) A dose–response curve of CA-0. The dotted line indicates the IC_{50} point of the chemical, which was 5.00 ±3.31 μM. (C) A strand transfer assay by radioisotope-labelled oligonuceotide. Lane 1 "N" stands for the negative control, with only a radioisotope-labelled nucleotide. Lane 2 "P" stands for positive control, with radioisotope-labelled nucleotide and recombinant integrase. Lanes 3 to 6 were with inhibitor. The open triangle and solid triangle indicate labelled oligonucelotide and strand transfer products, respectively.

©2005 International Medical Press

derivatives with different substituents. As demonstrated in Figure 2, all compounds had pyrrolo[3,4-c]carbazole structures as scaffolds, and all except CA-5, CA-10 and CA-19 had 2-dimethylaminoethyl group at position R2. Six of the 23 compounds demonstrated potent strand-transfer inhibition comparable to that of CA-0. These compounds were CA-1, CA-4, CA-8, CA-9, CA-12 and CA-13. IC_{50} values of these test compounds were similar with positive control S-1360. Moderate inhibitory activities were observed in twelve compounds, CA-2, CA-3, CA-7, CA-11, CA-14, CA-15, CA-16, CA-17, CA-18, CA-21, CA-22 and CA-23. Five compounds, CA-5, CA-6, CA-10, CA-19 and CA-20, did not show significant inhibition, even at the highest concentration tested

Figure 2. Structures of CA-0 and 23 carbazole derivatives evaluated for strand transfer inhibitory activity

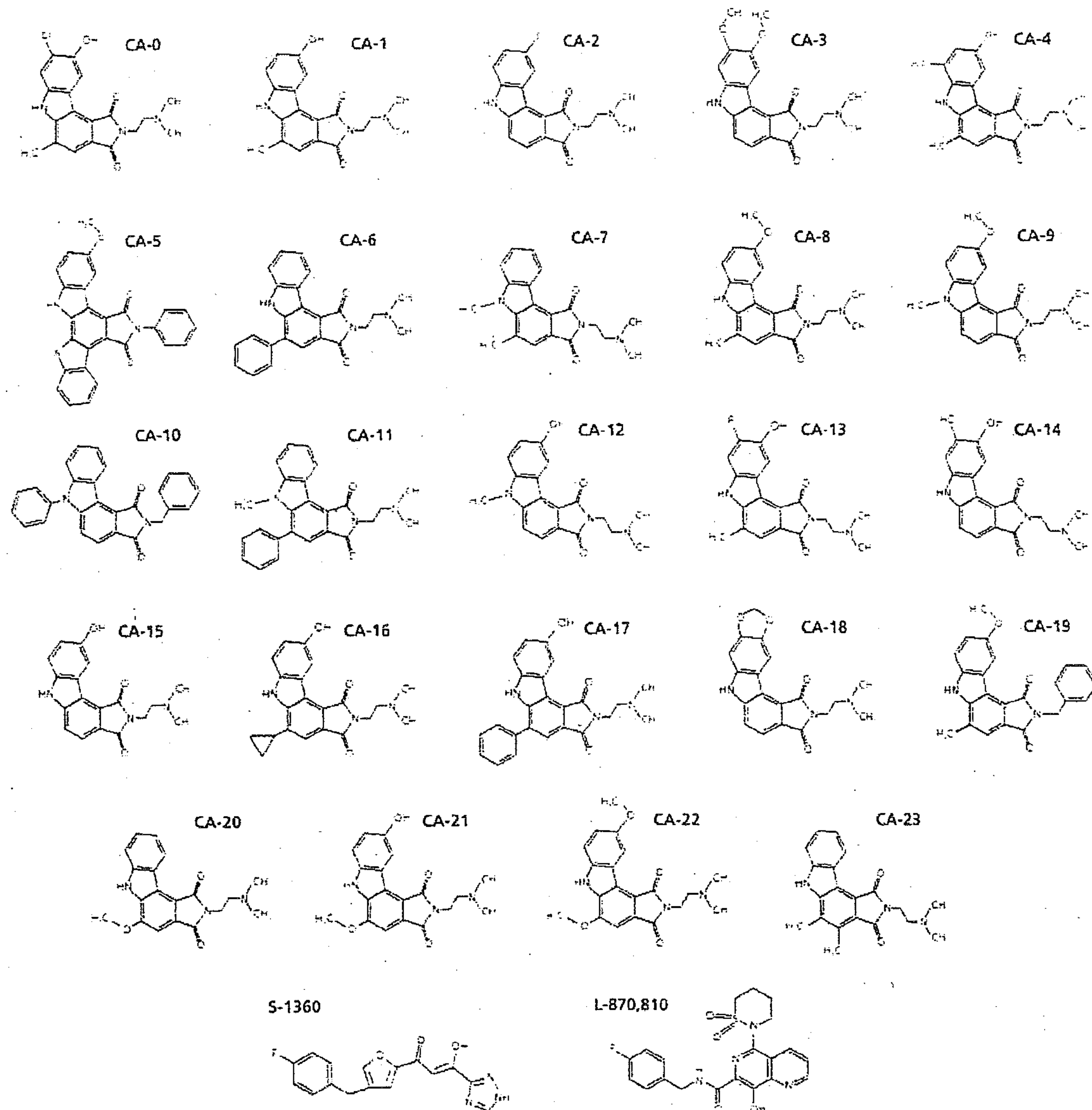

CA-0 and 23 related compounds with carbazole scaffold tested for strand-transfer inhibitory activities are depicted. S-1360 and L-870,810, which have previously been reported as potent IN inhibitors, are also shown.

(100 μM). The compounds that demonstrated potent strand-transfer inhibitory activity were also confirmed by gel-based assay, and IC_{50} values determined from the gel-based assay were consistent with the values determined via in-house plate assay (Table 1).

Carbazole derivatives are competitive inhibitors of integrase

To investigate the strand-transfer inhibitory mechanisms and kinetics of the compounds, we determined V_{max} and K_m of the inhibition by Lineweaver–Burke plot analyses. We selected two compounds, CA-0 and CA-13, for the analyses. As summarized in Table 2, larger K_m values (nM) were observed with higher inhibitory concentration, whereas V_{max} values (RU/min) did not change and remained consistent at any inhibitory concentration (Figure 3). As shown in Figure 3A and 3B, data-fitted lines of different time points converged on the Y axis, indicating that CA-0 and CA-13 inhibited strand-transfer in a competitive manner.

Table 1. Strand transfer and *in vitro* viral replication inhibitory activities of carbazole derivatives

	IC_{50} in strand transfer assay		Anti-HIV activity
	Plate assay (μM)	Gel assay (μM)	IC_{50} (μM)
(A) High-inhibitory group			
<u>CA-0</u>	5.00 ±3.31	1.24 ±0.09	0.48 ±0.06
CA-13	4.38 ±2.78	1.13 ±0.21	0.51 ±0.12
CA-1	7.94 ±4.12	2.97 ±0.21	0.92 ±0.15
CA-4	8.99 ±3.39	6.34 ±0.89	1.52 ±0.46
CA-8	6.61 ±4.17	6.38 ±0.32	0.79 ±0.07
CA-9	4.42 ±1.87	4.10 ±0.46	0.80 ±0.11
CA-12	5.93 ±3.53	3.14 ±0.04	0.69 ±0.15
(B) Intermediate-inhibitory group			
CA-2	22.50 ±2.27	ND	ND
CA-3	72.69 ±5.44	ND	ND
CA-7	11.88 ±7.66	ND	ND
CA-11	57.00 ±3.13	ND	ND
CA-14	17.37 ±1.79	ND	ND
CA-15	27.28 ±9.10	ND	ND
CA-16	20.51 ±15.11	ND	ND
CA-17	50.64 ±19.02	ND	ND
CA-18	10.68 ±8.88	ND	ND
CA-21	25.01 ±10.60	ND	ND
CA-22	16.92 ±7.32	ND	ND
CA-23	16.94 ±7.82	ND	ND
(C) Intermediate-inhibitory group			
CA-5	>100	ND	ND
CA-6	>100	ND	ND
CA-10	>100	ND	ND
CA-19	>100	ND	ND
CA-20	>100	ND	ND
(D) Previously reported inhibitor			
S-1360	4.67 ±1.89	ND	ND

Underline, indicates original compound. IC_{50}, 50% inhibition concentration; ND, not done

Carbazole derivates have not shown intercalative activity

Due to their planar structure and their manner of competitive inhibition, we were concerned that the compounds might have the intercalative activity to destroy substrate dsDNA, rather than binding to the IN to block its enzyme activity. To clear the possibility of the intercalation, EtBr displacement assay was carried out. Since EtBr intercalates into dsDNA and makes visualization possible by growing fluorescence under UV light, intercalative activity of the test compounds can be evaluated by whether the test compounds displace incorporated EtBr out from dsDNA. As shown in Figure 4, fluorescence intensity diminished in a dose-dependent manner by actinomycin D, a compound known as a potent intercalator. In contrast, our two test compounds CA-0 and CA-13 did not affect fluorescence intensity, even at the highest concentration of 1 mM, suggesting that CA-0 and CA-13 were not intercalators.

Antiviral activity

We employed a single replication infectivity assay using HeLa4.5/EGFP cells to investigate the potency of antiviral activity. IC_{50} values of CA-0 and the six compounds were 0.48, 0.92, 1.52, 0.79, 0.8, 0.69, 0.51 μM, respectively. The IC_{50} values of all seven compounds were 5.5 to 10.4-fold lower than that of the strand transfer assay (Table 1A). The discrepancy in IC_{50} between the two assays can be explained by stoichiometry of the inhibitor and the target enzyme in the two assays, and the estimated amount of IN in-strand transfer assay was higher than in the

Table 2. Inhibition kinetics of representative carbazole compounds CA-0 and CA-13

Chemical	Concentration	V_{max} (RU/min)	K_m (nM)
CA-0	10 μM	463.16 ±63.16	30.40 ±7.80
	5 μM	402.58 ±32.21	26.21 ±7.40
	1 μM	370.14 ±84.42	12.71 ±2.02
	0 μM	454.55 ±0.02	9.18 ±1.18
CA-13	10 μM	409.70 ±35.47	19.31 ±4.68
	5 μM	439.07 ±164.74	14.83 ±0.24
	1 μM	438.08 ±53.85	11.09 ±2.42
	0 μM	429.83 ±136.46	7.08 ±0.64

©2005 International Medical Press

Figure 3. Inhibition kinetics assays of two representative carbazole derivatives, CA-0 and CA-13

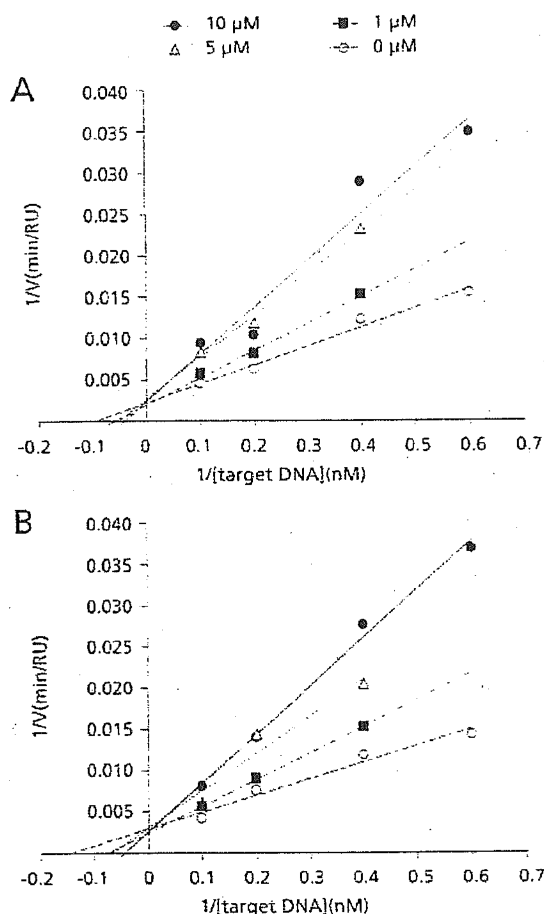

Lineweaver–Burke plot analyses of (A) CA-0 and (B) CA-13 are depicted.

Figure 4. Ethidium bromide displacement assays of two representative carbazole derivatives, CA-0 and CA-13

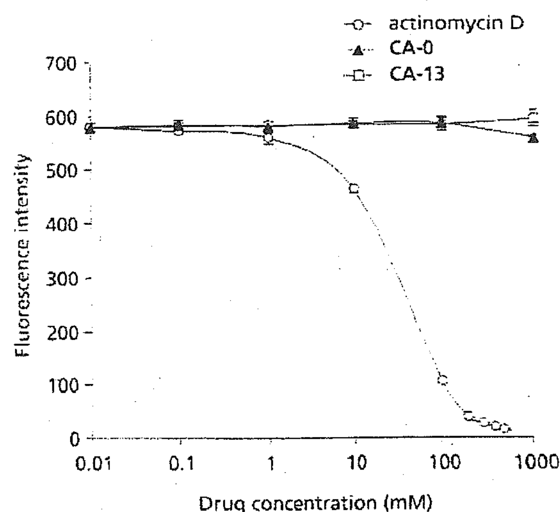

To evaluate intercalative activities of carbazole derivatives, ethidium bromide displacement assays were carried out for two representative compounds, CA-0 and CA-13.

HeLa4.5/EGFP assay. Seven compounds exhibited considerable toxicity, suggesting that efforts toward decreasing toxicity are necessary for the further development of carbazole-based inhibitors.

Discussion

Carbazole, a fused phenyl-ring structure with hydrophobicity, has provided an interesting scaffold for the development of novel drugs. Staurosporine, discovered among microbial alkaloids, was the first carbazole derivative reported to demonstrate biological activity (Omura *et al.*, 1977; Furusaki *et al.*, 1978; Furusaki *et al.*, 1982), which was protein kinase C inhibition (Tamaoki *et al.*, 1986). Other carbazole derivatives have demonstrated various other activities, such as topoisomerase inhibition (Marotto *et al.*, 2002; Facompre *et al.*, 2002; Carrasco *et al.*, 2001), hypotensive activity (Furusaki *et al.*, 1982), platelet aggregation inhibition (Oka *et al.*, 1986), and anti-fungal activity (Sunthitikawinsakul *et al.*, 2003). In this report we present another possible activity of carbazole derivatives, that of HIV-1 integrase inhibitor.

As compounds with three or four fused aromatic ring structures have been reported to demonstrate intercalative activity (Fukui & Tanaka, 1996; Dziegielewski *et al.*, 2002), we initially suspected that our carbazole derivatives also have intercalative activities, penetrating and disturbing target dsDNA, resulting in pseudo strand-transfer inhibition. Indeed, several carbazole derivatives have been recognized to demonstrate intercalative activity (Facompre *et al.*, 2002; Long *et al.*, 2002). We confirmed that actinomycin D, which is a well-known intercalator (Ross *et al.*, 1979; Wilson & Jones, 1982), demonstrated strand-transfer inhibition in our assay (data not shown). However, taking into consideration the data that our carbazole derivatives inhibited strand-transfer in a competitive manner, and also that the compounds could not displace EtBr out from dsDNA, we assume that our derivatives bind to part of the IN molecule, to the region responsible for DNA target

binding or to the catalytic site responsible for strand-transfer activity.

To understand in greater detail the substituents responsible for strand-transfer inhibitory activity, we analysed 23 carbazole derivatives, and classified them into three categories according to their levels of inhibition (Table 1). Six compounds were classified as the high-inhibition group, which demonstrated IC_{50} of less than 10 μM, 12 compounds were classified as the intermediate group, which demonstrated IC_{50} of greater than 10 μM and less than 100 μM, and five compounds were classified as the non-inhibition group, in which we did not observe significant inhibition even at the highest concentration tested (100 μM).

Comparing the compounds between and within these three categories, we recognized three factors responsible for strand-transfer inhibition. The first and most important factor is the incidence of a 2-dimethylaminoethyl group at position R2 (Figure 1A).

CA-8, which possesses a 2-dimethylaminoethyl group at position R2, demonstrated high inhibitory activity (IC_{50}: 6.61 ±4.17 μM), but **CA-19** (IC_{50}: >100 μM), which possesses a phenyl ring structure at the same R2 position, did not demonstrate inhibitory activity. Thus, it is clear that the incidence of a 2-dimethylaminoethyl group, which has a basic property, is critical for strand-transfer inhibition activity. Indeed, we recognized that all compounds in the "high-inhibitory group" and "intermediate-inhibitory group" had this basic substituent at position R2 (Table 1A, 1B, Figure 2). In contrast, three of five compounds in the "non-inhibitory group" had the phenyl ring structure at R2 position. It is thought that these compounds might bind to the acidic region on the IN molecule and compete with the target dsDNA.

The second factor is the incidence of a methyl (Me) group at position R5, R6 or R7. We recognized that compounds in the high inhibitory group had at least one Me group at the R5, R6 or R7 position (Table 1A, Figure 2). Comparing **CA-1** (IC_{50}: 7.94 ±4.12 μM), **CA-4** (IC_{50}: 8.99 ±3.39 μM), and **CA-12** (IC_{50}: 5.93 ±3.53 μM) with **CA-15** (IC_{50}: 27.28 ±9.10 μM), it is clear that the incidence of an Me group within the R5 to R7 positions was an important factor for enhanced inhibitory activity. It seems that the position of the substituent may not be critical between R5 and R6, as we did not see significant differences between **CA-1** (IC_{50}: 7.94 ±4.12 μM) and **CA-12** (IC_{50}: 5.93 ±3.53 μM), and also between **CA-8** (IC_{50}: 6.61 ±4.17 μM) and **CA-9** (IC_{50}: 4.42 ±1.87 μM).

According to the IC_{50} levels of **CA-5** (>100 μM), **CA-6** (>100 μM) and **CA-11** (>100 μM), it appears that bulky substituents at the R5 position have a negative effect on inhibition (Table 1C, Figure 2). Furthermore, the inhibition potential of the three compounds **CA-1** (IC_{50}: 7.94 ±4.12 μM), **CA-16** (IC_{50}: 20.51 ±15.11 μM) and **CA-17** (IC_{50}: 50.64 ±19.02 μM) depended on the molecular size of their R5 substituents. It is probable that the R5 substituents of these compounds were too large and that they interfered with surrounding molecules forming the binding site (Table 1A, 1B, Figure 2). These data indicate that the binding site of carbazole might have a space limitation, and thus the size and shape of the molecules may be important factors for inhibitor activity.

The third factor is the substituent at position R9. Comparing **CA-20** (IC_{50}: >100 μM), **CA-21** (IC_{50}: 25.01 ±10.60 μM) and **CA-22** (IC_{50}: 16.92 ±7.32 μM), these three compounds were identical, with the exception of the substituent at position R9 (Table 1B, 1C, Figure 2). **CA-21** and **CA-22** have hydroxyl residue and a methoxy group at position R9, respectively. We noticed a significant difference in inhibitory activity between **CA-20** and **CA-21**, and between **CA-20** and **CA-22**, suggesting the possibility that both the hydroxyl group and the methoxy group at R9 formed hydrogen bonds with the amino acid molecules forming the binding sites, as these two substituents have the potential to be hydrogen bond acceptors. It appears that hydroxyl and methoxy groups have similar effects on strand-transfer inhibitory activities. In addition to the above three factors, we found that molecular interaction between R8 and R9 substituents, and their arrangement, are also important determinants for efficient inhibitory activity. **CA-3**, with two methoxy groups at R8 and R9, appears to have a bulky arrangement of the two side chains, and demonstrated an IC_{50} of 72.69 ±5.44 μM, whereas **CA-14** and **CA-18**, which were expected to have horizontal arrangements, demonstrated lower IC_{50} values of 17.37 ±1.79 μM and 10.68 ±8.88 μM, respectively (Table 1B, Figure 2).

To summarize these structural elements, and to understand the common structure of molecules that demonstrated strand-transfer inhibitory activity, we superposed inhibitor structures having significant strand-transfer inhibition (**CA-0**, **CA-1**, **CA-4**, **CA-8**, **CA-9**, **CA-12** and **CA-13**) (Figure 5A), and the structures of compounds with no inhibition (**CA-5**, **CA-6**, **CA-10**, **CA-19** and **CA-20**) (Figure 5B). In comparing these two overlapped figures, we found that the compounds with inhibitory activity share a largely identical structure and similar molecular size. In contrast, the non-inhibitory compounds had larger and more uneven-shaped side chains. Overall, the superposed structures indicate that the molecules should be planar and have basic diethylaminoethyl groups to demonstrate strand-transfer inhibitory activity.

In conclusion, we have identified a small molecular weight compound with a carbazole scaffold, which can be the lead compound for developing novel IN inhibitors. Furthermore, analysing the IN inhibitory mechanisms of

©2005 International Medical Press

Figure 5. A structural comparison between high/intermediate inhibitory compounds and non-inhibitory compounds

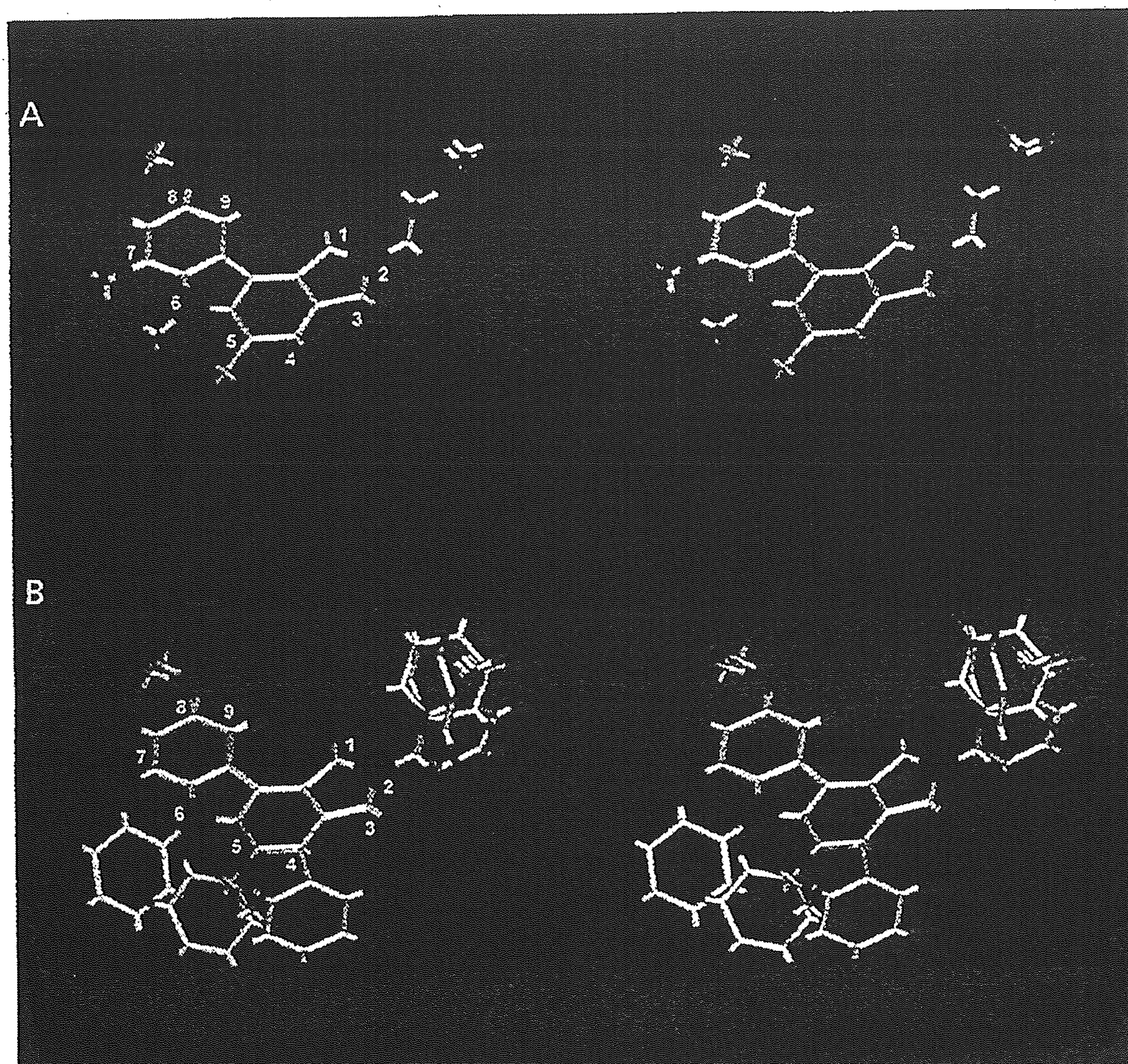

Superposed structures of (A) five non-inhibitory compounds, CA-5, 6, 10, 19 and 20, and (B) seven inhibitory compounds, CA-0, 1, 4, 8, 9, 12 and 13, are demonstrated in stereo-view images. In both figures, residue numbers are indicated beside the structures. Red, dark blue and light blue indicate oxygen, nitrogen and hydrogen molecules, respectively. Green indicates chlorine or fluorine molecules. SYBYL software Version 6.9.1 running on an SGI Fuel workstation was used to construct the figures.

carbazole derivatives may yield more detailed information regarding HIV-1 IN structure and function.

Acknowledgements

This study was supported by a grant from the Human Sciences Foundation, the Organization of Pharmaceutical Safety and Research of Japan and the Ministry of Health, Labor and Welfare of Japanese Government. This study was partly supported by the Program for Promotion of Fundamental Studies in Health Sciences of the National Institute of Biomedical Innovation (NIBIO).

We would like to thank Dr. Haruo Tanaka and Takuro Shiomi, professor and associate professor of Kitazato

Institute, for their valuable advice and comments. We would also like to thank the laboratory members of Toyama Chemical Co. Ltd. for supplying the compounds in the study. Finally, we would like to thank Ms. Mary Phillips and Ms. Yumi Fujiuji for preparing the manuscript.

References

Balzarini J (2004) Current status of the non-nucleoside reverse transcriptase inhibitors of human immunodeficiency virus type 1. *Current Topics in Medicinal Chemistry* **4**:921–944.

Burke CJ, Sanyal G, Bruner MW, Ryan JA, LaFemina RL, Robbins HL, Zeft AS, Middaugh CR & Cordingley MG (1992) Structural implications of spectroscopic characterization of a putative zinc finger peptide from HIV-1 integrase. *The Journal of Biological Chemistry* **267**:9639–9644.

Cain BF, Baguley BC & Denny WA (1978) Potential antitumor agent. 28. deoxyribonucleic acid polyintercalating agents. *Journal of Medicinal Chemistry* **21**:658–668.

Carrasco C, Vezin H, Wilson WD, Ren J, Chaires JB & Bailly C (2001) DNA binding properties of the indolocarbazole antitumor drug NB-506. *Anticancer Drug Design* **16**:99–107.

Chun TW, Finzi D, Margolick J, Chadwick K, Schwartz D & Siliciano RF (1995) *In vivo* fate of HIV-1-infected T cells: quantitative analysis of the transition to stable latency. *Nature Medicine* **1**:1284–1290.

Craigie R, Hickman AB & Engelman A (1995) Integrase. in *HIV: A Practical Approach – Volume 2: Biochemistry, Molecular Biology, and Drug Discovery*, pp. 53–71. Edited by J Karn. New York: Oxford University Press.

Dayam R & Neamati N (2003) Small-molecule HIV-1 integrase inhibitors: the 2001–2002 update. *Current Pharmacology Design* **9**:1789–1802.

De Clercq E (1992) HIV inhibitors targeted at the reverse transcriptase. *AIDS Research and Human Retroviruses* **8**:119–134.

Dziegielewski J, Slusarski B, Konitz A, Skladanowski A & Konopa J (2002) Intercalation of imidazoacridinones to DNA and its relevance to cytotoxic and antitumor activity. *Biochemical Pharmacology* **63**:1653–1662.

Engelman A & Craigie R (1992) Identification of conserved amino acid residues critical for human immunodeficiency virus type 1 integrase function *in vitro*. *Journal of Virology* **66**:6361–6369.

Engelman A, Englund G, Orenstein JM, Martin MA & Craigie R (1995) Multiple effects of mutations in human immunodeficiency virus type 1 integrase on viral replication. *Journal of Virology* **69**:2729–2736.

Engelman A, Hickman AB & Craigie R (1994) The core and carboxyl-terminal domains of the integrase protein of human immunodeficiency virus type 1 each contribute to nonspecific DNA binding. *Journal of Virology* **68**:5911–5917.

Facompre M, Carrasco C, Colson P, Houssier C, Chisholm JD, Van Vranken DL & Bailly C (2002) DNA binding and topoisomerase I poisoning activities of novel disaccharide indolocarbazoles. *Molecular Pharmacology* **62**:1215–1227.

Fukui K & Tanaka K (1996) The acridine ring selectively intercalated into a DNA helix at various types of abasic sites: double strand formation and photophysical properties. *Nucleic Acids Research* **24**:3962–3967.

Furusaki A, Hashiba N, Matsumoto T, Hirano A, Iwai Y & Omura S (1978) X-ray crystal structure of staurosporine: a new alkaloid from a Streptomyces strains. *Journal of the Chemical Society Chemical Communication* 800–801.

Furusaki A, Hashiba N, Matsumoto T, Hirano A, Iwai Y & Omura S (1982) The crystal and molecular structure of staurosporine, a new alkaloid from a Streptomyces strains. *Bulletin of the Chemical Society of Japan* **55**:3681–3685.

Goldgur Y, Craigie R, Cohen GH, Fujiwara T, Yoshinaga T, Fujishita T, Sugimoto H, Endo T, Murai H & Davies DR (1999) Structure of the HIV-1 integrase catalytic domain complexed with an inhibitor: a platform for antiviral drug design. *Proceedings of the National Academy of Sciences, USA* **96**:13040–13043.

Grobler JA, Stillmock K, Hu B, Witmer M, Felock P, Espeseth AS, Wolfe A, Egbertson M, Bourgeois M, Melamed J, Wai JS, Young S, Vacca J & Hazuda DJ (2002) Diketo acid inhibitor mechanism and HIV-1 integrase: implications for metal binding in the active site of phosphotransferase enzymes. *Proceedings of the National Academy of Sciences USA* **99**:6661–6666.

Hazuda DJ, Anthony NJ, Gomez RP, Jolly SM, Wai JS, Zhuang L, Fisher TE, Embrey M, Guare JP, Jr., Egbertson MS, Vacca JP, Huff JR, Felock PJ, Witmer MV, Stillmock KA, Danovich R, Grobler J, Miller MD, Espeseth AS, Jin L, Chen IW, Lin JH, Kassahun K, Ellis JD, Wong BK, Xu W, Pearson PG, Schleif WA, Cortese R, Emini E, Summa V, Holloway MK & Young SD (2004) A naphthyridine carboxamide provides evidence for discordant resistance between mechanistically identical inhibitors of HIV-1 integrase. *Proceedings of the National Academy of Sciences USA* **101**:11233–11238.

Hazuda DJ, Felock P, Witmer M, Wolfe A, Stillmock K, Grobler JA, Espeseth A, Gabryelski L, Schleif W, Blau C & Miller MD (2000) Inhibitors of strand transfer that prevent integration and inhibit HIV-1 replication in cells. *Science* **287**:646–650.

Imamichi T (2004) Action of anti-HIV drugs and resistance: reverse transcriptase inhibitors and protease inhibitors. *Current Pharmaceutical Design* **10**:4039–4053.

Johnson AA, Marchand C & Pommier Y (2004) HIV-1 integrase inhibitors: a decade of research and two drugs in clinical trial. *Current Topics in Medicinal Chemistry* **4**:1059–1077.

Khan E, Mack JP, Katz RA, Kulkosky J & Skalka AM (1991) Retroviral integrase domains: DNA binding and the recognition of LTR sequences. *Nucleic Acids Research* **19**:851–860.

Kohl NE, Emini EA, Schleif WA, Davis LJ, Heimbach JC, Dixon RA, Scolnick EM & Sigal IS (1988) Active human immunodeficiency virus protease is required for viral infectivity. *Proceedings of National Academy of Sciences USA* **85**:4686–4690.

LaFemina RL, Schneider CL, Robbins HL, Callahan PL, LeGrow K, Roth E, Schleif WA & Emini EA (1992) Requirement of active human immunodeficiency virus type 1 integrase enzyme for productive infection of human T-lymphoid cells. *Journal of Virology* **66**:7414–7419.

Long BH, Rose WC, Vyas DM, Matson JA & Forenza S (2002) Discovery of antitumor indolocarbazoles: rebeccamycin, NSC 655649, and fluoroindolocarbazoles. *Current Medicinal Chemistry. Anti-Cancer Agents* **2**:255–266.

Marotto A, Kim YS, Schulze E & Pindur U (2002) New indolocarbazoles as antitumour active compounds: evaluation of the target by experimental and theoretical studies. *Pharmazie* **57**:194–197.

Oka S, Kodama M, Takeda H, Tomizuka N & Suzuki H (1986) Staurosporine, a potent platelet aggregation inhibitor form a *Streptomyces* species. *Agricultural and Biological Chemistry* **50**:2723–2727.

Omura S, Iwai Y, Hirano A, Nakagawa A, Awaya J, Tsuchiya H, Takahashi Y & Masuma R (1977) A new alkaloid AM-2282 of *Streptomyces* origin. Taxonomy, fermentation, isolation and preliminary characterization. *The Journal of Antibiotics (Tokyo)* **30**:275–282.

©2005 International Medical Press

Pluymers W, Pais G, Van Maele B, Pannecouque C, Fikkert V, Burke TR, Jr., De Clercq E, Witvrouw M, Neamati N & Debyser Z (2002) Inhibition of human immunodeficiency virus type 1 integration by diketo derivatives. *Antimicrobial Agents and Chemotherapy* **46**:3292–3297.

Pommier Y, Marchand C & Neamati N (2000) Retroviral integrase inhibitors year 2000: update and perspectives. *Antiviral Research* **47**:139–148.

Ross WE, Glaubiger D & Kohn KW (1979) Qualitative and quantitative aspects of intercalator-induced DNA strand breaks. *Biochimica et Biophysica Acta* **562**:41–50.

Ruscetti FW (1985) Immunopathology associated with human lymphotropic retroviruses. *Survey and Synthesis of Pathology Research* **4**:216–226.

Schauer M & Billich A (1992) The N-terminal region of HIV-1 integrase is required for integration activity, but not for DNA binding. *Biochemical and Biophysical Research Communications* **185**:874–880.

Sunthitikawinsakul A, Kongkathip N, Kongkathip B, Phonnakhu S, Daly JW, Spande TF, Nimit Y & Rochanaruangrai S (2003) Coumarins and carbazoles from *Clausena excavata* exhibited antimycobacterial and antifungal activities. *Planta Medica* **69**:155–157.

Tamaoki T, Nomoto H, Takahashi I, Kato Y, Morimoto M & Tomita F (1986) Staurosporine, a potent inhibitor of phospholipid/Ca++ dependent protein kinase. *Biochemical and Biophysical Research Communications* **135**:397–402.

Tronchet JM & Seman M (2003) Non-nucleoside inhibitors of HIV-1 reverse transcriptase: from the biology of reverse transcription to molecular design. *Current Topics in Medicinal Chemistry* **3**:1496–1511.

Wilson WD & Jones RL (1982) Interaction of actinomycin D, ethidium, quinacrine, daunorubicin, and tetralysine with DNA: 31P NMR chemical shift and relaxation investigation. *Nucleic Acids Research* **10**:1399–1410.

Woerner AM & Marcus-Sekura CJ (1993) Characterization of a DNA binding domain in the C-terminus of HIV-1 integrase by deletion mutagenesis. *Nucleic Acids Research* **21**:3507–3511.

Received 22 August 2005, accepted 27 September 2005